Research

New Phytologist

Negative allometry of leaf xylem conduit diameter and double-wall thickness: implications for implosion safety

Ilaine Silveira Matos[1,2], Samantha McDonough[1], Breanna Carrillo Johnson[1], Diana Kalantar[1], James Rohde[1], Roshni Sahu[1], Joyce Wang[1], Adrian Fontao[1], Jason To[1], Sonoma Carlos[1], Lisa Garcia[3], Mickey Boakye[1], Holly Forbes[4] and Benjamin Wong Blonder[1]

[1]Department of Environmental Science, Policy, and Management, University of California Berkeley, Berkeley, CA 94720, USA; [2]School of Biological Sciences, The University of Adelaide, Adelaide, SA, 5005, Australia; [3]Department of Biology, University of New Mexico, Albuquerque, NM 87131, USA; [4]University of California Botanical Garden, Berkeley, CA 94720, USA

Author for correspondence:
Ilaine Silveira Matos
Email: ilaine.matos@gmail.com

Received: *11 December 2023*
Accepted: *25 March 2024*

New Phytologist (2024) **242:** 2464–2478
doi: 10.1111/nph.19771

Key words: drought, implosion safety, leaf anatomy, plant allometry, plant hydraulics, xylem collapse, xylem conduit.

Summary

- Xylem conduits have lignified walls to resist crushing pressures. The thicker the double-wall (*T*) relative to its diameter (*D*), the greater the implosion safety. Having safer conduits may incur higher costs and reduced flow, while having less resistant xylem may lead to catastrophic collapse under drought. Although recent studies have shown that conduit implosion commonly occurs in leaves, little is known about how leaf xylem scales *T* vs *D* to trade off safety, flow efficiency, mechanical support, and cost.
- We measured *T* and *D* in > 7000 conduits of 122 species to investigate how *T* vs *D* scaling varies across clades, habitats, growth forms, leaf, and vein sizes.
- As conduits become wider, their double-cell walls become proportionally thinner, resulting in a negative allometry between *T* and *D*. That is, narrower conduits, which are usually subjected to more negative pressures, are proportionally safer than wider ones. Higher implosion safety (i.e. higher *T*/*D* ratios) was found in asterids, arid habitats, shrubs, small leaves, and minor veins.
- Despite the strong allometry, implosion safety does not clearly trade off with other measured leaf functions, suggesting that implosion safety at whole-leaf level cannot be easily predicted solely by individual conduits' anatomy.

Introduction

Vascular plants developed lignified xylem conduits to transport water with high efficiency (Sperry, 2003) but variable safety (Hacke *et al.*, 2001). Plants can experience extreme negative pressures inside the xylem, which increases the risk of conduit dysfunction by either cavitation (i.e. rupture of the continuous water columns due to the formation and expansion of air bubbles) or implosion (i.e. the collapse of conduit walls due to compression forces) (Hacke *et al.*, 2004; Sperry & Hacke, 2004). For a long time, physiological work on xylem dysfunction focused on cavitation as the main process reducing hydraulic efficiency under drought (e.g. Brodribb & Holbrook, 2005; Choat *et al.*, 2012). It was assumed that cavitation occurs long before water potential falls sufficiently low to collapse cells (Hacke *et al.*, 2001; Sperry & Hacke, 2004; Pittermann *et al.*, 2011). However, several studies have now showed that implosion commonly occurs in leaves of conifers (e.g. Cochard *et al.*, 2004; Zhang *et al.*, 2014; Chin *et al.*, 2022), ferns, and angiosperms (Zhang *et al.*, 2016, 2023). At least in the smaller leaf conduits (minor veins), reversible implosion preempts cavitation and influences whole-leaf responses to water stress (Cochard *et al.*, 2004; Zhang *et al.*, 2016, 2023). Implosion was observed at leaf water potentials (Ψ_{leaf}) as high as −0.9 MPa, suggesting that conduits might not be as resistant to implosion as previously thought (Zhang *et al.*, 2023). Thus, there is a need to better understand leaf features dictating implosion safety and how it varies across species.

Implosion occurs when radial (force orientated toward the conduit center) or hoop forces (force exerted around the conduit circumference) create mechanical stress that exceeds the wall strength, so it buckles inwards. Diverse traits, such as conduit shape, length, and elasticity, influence how much tension can be supported before a conduit implodes (Sperry & Hacke, 2004). However, to a first approximation, implosion safety at the conduit level can be described as a monotonic function of the ratio between conduit double-wall thickness (*T* = the thickness of the conduit cell wall plus the thickness of the adjacent conduit wall) and its maximum lumen diameter (*D* = the longest diameter of the conduit), that is *T*/*D* also called 'thickness-to-span' ratio (Hacke *et al.*, 2001; Sperry *et al.*, 2006). Sometimes implosion safety is also modeled as $(T/D)^2$ (Hacke *et al.*, 2001) or $(T/D)^3$ (Blackman *et al.*, 2010). Regardless of the exponent, this relationship implies that implosion safety can increase by either narrowing or thickening conduits. Either way may result in functional disadvantages (Blackman *et al.*, 2010; Pratt & Jacobsen, 2017), even if there is some nonlinearity in the relationship between *T*, *D*, and *T*/*D*. Narrowing conduits decreases flow efficiency. According to the Hagen–Poiseuille law, the efficiency of

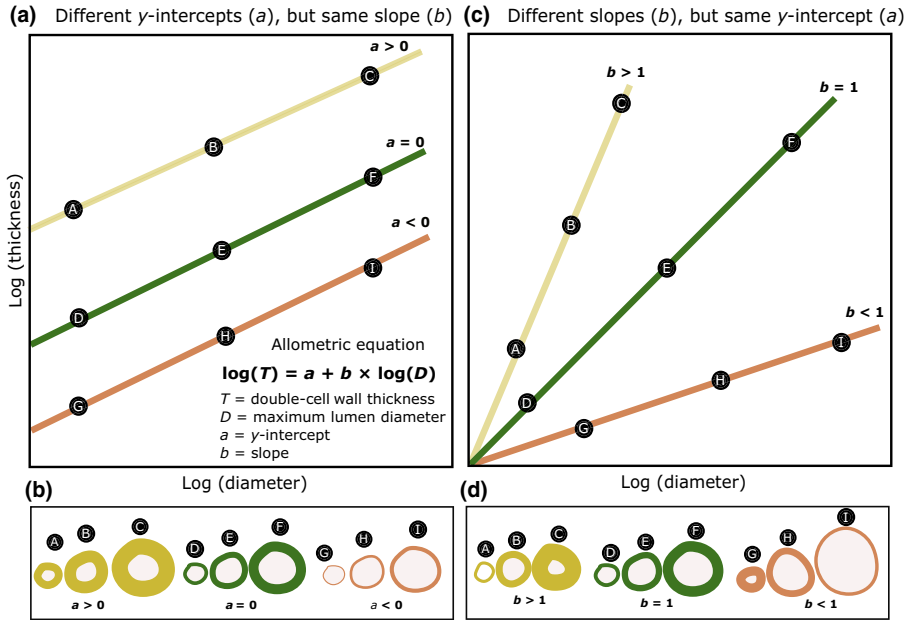

Fig. 1 Scaling scenarios for the log–log relationship between leaf conduit double-wall thickness (T) and maximum lumen diameter (D) for three hypothetical species (yellow, green, and orange). (a) Species have same slope (b coefficient) but different y-intercepts (a coefficients): $a > 0$ (yellow line) – conduits have thicker cell walls relative to their diameter (i.e. higher lignification), potentially resulting in higher implosion safety across the entire venation network; $a = 0$ (green line) – conduits have lower degree of lignification; $a < 0$ (orange line) – conduits have thinner cells walls relative to their diameter, potentially resulting in lower implosion safety across the entire leaf venation network. (b) Illustrations of how conduits T and D are expected to vary across vein sizes in each of the three scaling scenarios with same b but different a. (c) Species have same a but different b: $b > 1$ (yellow line) – as conduits become wider their cell walls become proportionally thicker, resulting in greater xylem reinforcement and lower vulnerability to implosion in wider conduits; $b = 1$ (green line) – conduits diameter and thickness increase proportionally, resulting in a constant safety implosion across conduits of different diameters; $b < 1$ (orange line) – as conduits become wider their cell walls become proportionally thinner, resulting in greater xylem reinforcement in narrower conduits, but potentially higher vulnerability to implosion in wider conduits. (d) Illustrations of how conduits T and D are expected to vary across vein sizes in each of the three scaling scenarios of same a but different b.

transport in a pipe increases to the fourth power of its diameter, so any small reduction in diameter implies a great decline in flow (Tyree *et al.*, 1994). Thickening conduits increases construction cost. Although thicker conduits are safer against implosion and more mechanically supported (Růžička *et al.*, 2015), they are also more costly to produce because lignin is an expensive polymer to biosynthesize (Amthor, 2003).

Therefore, plants must trade off implosion safety and mechanical support vs maximum efficiency at a minimum cost (Sperry, 2003; Sperry *et al.*, 2006; Pratt & Jacobsen, 2017). Assuming linear trade-offs exist between those functions, we can use a linear equation $\log(T) = a + b \times \log(D)$ to investigate how xylem conduits coordinate their growth in diameter (due to cell enlargement) and in thickness (due to lignin deposition) to trade off among different functions (Fig. 1). The y-intercept (a coefficient) indicates the overall leaf implosion resistance, with higher values suggesting thicker cell walls (higher degree of lignification) for any given conduit diameter, and hence higher implosion safety across the entire network (i.e. from the petiole all the way to the minor veins; Fig. 1a,b). The slope (b coefficient) indicates how the implosion safety varies across vein spatial scales, that is across vein orders (Fig. 1c,d). If $b = 1$ (isometric allometry), then conduits scale T proportionally to D, that is as conduits become wider their cell walls become proportionally thicker, resulting in a level of conduit reinforcement (T/D) that is constant across different vein orders. If $b > 1$ (positive allometry), narrower conduits have relatively thinner cell walls than wider conduits do. In this case, narrower conduits have lower implosion safety, while wider conduits are mechanically stronger and safer against implosion, but also more costly to produce. If $b < 1$ (negative allometry), narrower conduits have relatively thicker cell walls than wider conduits do. In this case, narrower conduits might have higher implosion safety, while wider conduits might be less costly to produce and more efficient, but at the expense of being potentially more vulnerable to implosion. Therefore, a indicates the implosion safety of the whole network (when $b = 1$), whereas b indicates how implosion safety varies from wider to narrower conduits.

Because xylem tension increases from the petiole to the minor veins, there could be a gradient in implosion safety from the proximal to distal ends of the venation network. That is, because minor veins are subjected to more negative water potentials and thus are under higher risk of collapse, we could expect them to develop higher implosion safety than major veins, resulting in $b < 1$. Assuming that the xylem path length shapes the water potential drop across the leaf, then we could also expect higher implosion resistance in terminal veins as leaf increases in size. Alternatively, minor veins may exhibit lower implosion safety. The greater diffusivity of minor veins, often achieved by the presence of more or larger pit pores, permit greater radial leakage to

the mesophyll (Zwieniecki *et al.*, 2002), but may also weaken the double-cell walls (Hacke *et al.*, 2004; Sperry & Hacke, 2004), reducing their implosion resistance. Studies investigating implosion safety variation across vein orders have found inconsistent results, either showing no variation in the T vs D scaling across vein orders (Blackman *et al.*, 2018) or showing that implosion occurs first in the minor veins (Zhang *et al.*, 2016, 2023). Therefore, it is still unclear whether there is any generality in how T and D scale across vein orders and leaf sizes.

Similarly, species from arid habitats experience more xylem tension and are likely under greater selection for developing safer conduits (Blackman *et al.*, 2018; Echeverría *et al.*, 2022; Nardini, 2022). But, it is unclear whether their higher implosion safety is achieved by developing more lignified xylem conduits across the entire leaf network (higher a), by investing in safer minor veins ($b < 1$), or by a combination of both. Previous studies evaluating those questions have focused on stem xylem (e.g. Pittermann *et al.*, 2006; Echeverría *et al.*, 2022). Because leaf veins can be substantially less lignified than stem conduits, it is unclear whether the findings observed in wood xylem can also be applied to leaves. Some studies investigated T vs D scaling in leaf xylem of a subset of gymnosperms (Pittermann *et al.*, 2011), angiosperms (e.g. Blackman *et al.*, 2018), and ferns species (Pittermann *et al.*, 2011). However, we still lack a more comprehensive assessment of leaf implosion safety in a wide range of phylogenetically and morphologically diverse species.

Here, we investigated how implosion safety varied in 122 ferns and angiosperms species with different habitats, growth forms, and leaf sizes. For each species, we also measured traits describing leaf mechanical support, flow efficiency, and construction cost and tested for potential trade-offs between them. Specifically, we asked the following: (1) How do leaf conduits' T and D scale to each other? (2) How do the coefficients (a and b) of the T vs D scaling vary across species, clades, habitats, growth forms, leaf sizes, and vein orders? (3) Is there a linear trade-off between implosion safety vs mechanical support, flow efficiency, and construction cost?

Materials and Methods

Study species

We sampled 122 species (Supporting Information Table S1) from the University of California Botanical Garden at Berkeley (' UCBG', 37.87, −122.23; Berkeley, CA, USA). Species selection maximized phylogenetic coverage, and included species with different growth forms, leaf sizes, and habitats (Table S1; Fig. S1). Because this garden collection often has a single or just a few individuals per species, our sampling approach was limited to a few branches (> 1 m long) collected from a single individual (woody species), or to a few leaves collected from 1 to 5 individuals (herbaceous species). Samples were collected in the morning, re-cut under water, re-hydrated overnight, and then used for the measurement of leaf anatomical and functional traits. As most of those traits are destructive, we used different leaves for each trait. This sampling approach with a low number of replicates within species is appropriate for studying inter-specific trait variation across a phylogenetically diverse set of species (Shipley *et al.*, 2016).

Anatomical measurements

Fresh and mature leaves (3–4 per species) were cut into 1-cm^2 sections, fixed in formalin acetic acid, and embedded in paraffin blocks. Sections included different leaf portions (base, middle, apex, and petiole) and vein orders. Transverse cross sections of 8–10 μm of thickness were cut with a microtome (RM2265; Leica, Nubloch, Germany), stained using the Johansen's safranin-O and fast green method (Johansen, 1940), and mounted in permanent glass slides using Cytoseal 60 medium (Richard-Allan Scientific, San Diego, CA, USA). Sections were observed under a light microscope (DM 2000; Leica), and photographed (at ×20–100 objectives) with a camera control unit (DS-Fi1; Nikon, Melville, NY, USA). We selected 6–8 images per species and manually measured the maximum and minimum lumen diameters (D_{max} and D_{min}, μm) and the double-cell wall thickness (T, μm) on all or, at most, 10 adjacent conduits per image using ImageJ (https://imagej.nih.gov/). In vascular bundles with > 10 conduits, we systematically selected conduits to cover the range of conduit sizes observed in each picture.

Functional traits

Implosion safety ratio (T/D) was calculated as the ratio between T and D_{max} for each conduit. Higher T/D values are assumed to be associated with greater implosion safety. Per this assumption, we estimated a theoretical critical implosion pressure (P_{cri}, MPa), that is the critical pressure above which a cell wall collapses. P_{cri} should be a function of T/D, but the specific equation depends on what type of stress (radial or hoop) induces the implosion (Young, 1989). Because the prevalent type of stress causing leaf conduits to collapse is not known precisely, we used two different mechanical models of P_{cri}.

The first model Eqn 1 (Blackman *et al.*, 2010) is based on Timoshenko's equation for an isolated and perfectly rounded pipe under negative pressure (Timoshenko, 1930) and considers that hoop forces are the main underlying stress inducing collapse.

$$P_{cri1} = \frac{2E}{(1-\upsilon^2)} \times \left(\frac{T}{2D_{max}}\right)^3 \quad \text{Eqn 1}$$

where, E, radial elastic modulus of xylem conduits in MPa; υ, Poisson ratio for lignin = 0.28; T, conduit double-wall cell thickness in μm; D_{max}, maximum conduit diameter in μm.

In the absence of per species data, P_{cri1} was calculated assuming that E ranges from 100 (P_{cri1} low) to 300 MPa (P_{cri1} high) (Blackman *et al.*, 2010). To estimate how much the leaf conduits cross-sectional shape deviates from a rounded shape, we calculate the conduit ovality as $O = (D_{max} - D_{min})/(D_{max} + D_{min})$, where D_{min} is the minimum conduit lumen diameter in μm (Ikeda *et al.*, 2013). An ovality value of 0 indicates a perfectly rounded

conduit. Conduits with $O < 0.005$ still behave as a cylindrical pipe under compressive forces, but above this value conduit shape starts interfering in P_{cri1} (Ikeda *et al.*, 2013). Note that O was not directly used to adjust P_{cri1}.

The second model Eqn 2 (Hacke *et al.*, 2001; Sperry & Hacke, 2004) considers the double-wall between neighboring conduits as a flat solid plate of finite D_{max} and effectively infinite length. It also assumes that radial stresses occurring in the common wall between an embolized and a water-filled conduit are the main cause of implosion, while hoop stresses are negligible (Sperry & Hacke, 2004).

$$P_{cri2} = \left(\frac{W}{b}\right) \times \left(\frac{T}{D_{max}}\right)^2 \quad \text{Eqn 2}$$

where, W, cell wall strength at saturation in MPa; b, coefficient that depends on the width-to-length ratio of the conduits (0.25 for a ratio of 0.5 or less).

Cell wall strength is unknown for the species evaluated. In wood xylem, W *c.* 40–80 MPa (Hacke *et al.*, 2001; Sperry & Hacke, 2004), but it could be lower for leaf xylem. Therefore, we calculated P_{cri2} assuming that W ranges from 10 (P_{cri2} low) to 80 MPa (P_{cri2} high). Although both mechanical models described above are approximations (Hacke *et al.*, 2004; Sperry & Hacke, 2004) and may not give accurate pressures for collapse, they likely account for enough variation across species to provide useful insights.

Flow efficiency was quantified as the maximum leaf hydraulic conductance ($Kleaf_{max}$, mmol m^{-2} s^{-1} MPa^{-1}), measured on 4–10 leaves per species using the evaporative flux method (Sack & Scoffoni, 2012) with a pressure-drop flow meter (Melcher *et al.*, 2012). In this method, a transpiring leaf was firmly connected to a tube running to a water source, which was then placed in series with a resistance tube (PEEK tubing; VWR, Radnor, PA, USA) of known hydraulic conductance. To accelerate the evaporation process, leaf samples were placed over a box fan and below a light source. Once a steady-state flow rate was achieved, pressures across the resistance tube were recorded, for at least 10 min, using two pressure transducers (model PX26-001GV; Omega Engineering, Norwalk, CT, USA) interfaced to a data logging system (U6 USB; Labjack, Lakewood, CO, USA). Next, the leaf was disconnected from the tubing system, and placed in a sealable plastic bag for *c.* 20 min for water potential equilibration. Final leaf water potential was measured using a pressure chamber (model 1505D; PMS, Albany, OR, USA). Leaf area (LA, cm^2) was obtained using a flatbed scanner and the leafarea macro (https://github.com/bblonder/leafarea) in the ImageJ software v.1.53t (https://imagej.nih.gov/). Finally, $Kleaf_{max}$ normalized by leaf area and corrected for leaf temperature was calculated following Sack & Scoffoni (2012). $Kleaf_{max}$ describes how much water flows across the leaf in response to a water potential gradient between the leaf and the surrounding atmosphere; hence, higher values indicate higher flow efficiency. LA obtained as above, was used to classify species as microphyllous ($LA \leq 20.25$ cm^2), mesophyllous ($20.25 < LA < 45$ cm^2), and macrophyllous ($LA \geq 45$ cm^2), following Webb (1959).

Mechanical support was quantified as the leaf flexural modulus of elasticity (ε, MN m^{-2}). To obtain ε, we performed 3-point bending tests using a Universal Testing Machine (Test stand ES30; Mark-10, Copiague, NY, USA) on 3–4 leaves per species. Leaves were placed in the UTM machine with their longitudinal axis parallel to the bending fixture. During the bending test, the force (force gauges M5-5 and M5-20; Mark-10) and the displacement (travel display ESM0001; Mitutoyo, Aurora, IL, USA) were recorded, and then used to produce force-displacement plots. After each test, leaf width and thickness at the bending point and the span length between the two bending fixtures were measured with a digital caliper, and then used for the calculation of ε following Read *et al.* (2005). Higher values of ε (i.e. stiffer leaves) indicate higher mechanical support. In 14 species (Table S1), leaves were too small to be properly attached to the bending fixture and/or too flexible to produce detectable bending forces, so ε was not measured.

Construction cost was estimated using two different proxies: leaf mass per area (LMA, g m^{-2}) and total volume of veins per area (VTotV, mm^3 mm^{-2}). LMA describes the total amount of resources invested in constructing each unit of leaf area. To obtain LMA, 3–5 leaves per species were scanned to obtain the leaf area and oven-dried at 50°C for 48 h to determine their dry mass. LMA was then calculated as leaf dry mass divided by leaf area (Pérez-Harguindeguy *et al.*, 2016). VTotV describes the total volume of veins per unit of leaf area, and it is a reasonable proxy of the construction cost of conduits *per se*. To calculate VTotV, we first obtained leaf cleared images of all species, except for *Nymphaea* spp. and *Aucuba japonica* Thunb., because it was impossible to obtain a clear image of their venation networks. Next, we used the LeafVeinCNN app in MATLAB to calculate the total volume of veins (Xu *et al.*, 2021), assuming that veins have a cylindrical shape. Finally, we divided the total volume of veins by leaf area to obtain VTotV. Higher LMA and VTotV values reflect higher construction cost.

Species habitat

We inferred habitat for each species based on its current geographic range. To retrieve the geographic range, we used occurrence data from Botanical Information and Ecology Network (Maitner *et al.*, 2018) and Global Biodiversity Information Facility (https://www.gbif.org/) databases. Occurrence records were manually cleaned by removing duplicated, outdated (pre-1950), or suspect geographical coordinates (outside the species natural habitat). Next, the mean annual precipitation (MAP) for each coordinate was extracted from the Worldclim database (https://www.worldclim.org/data/bioclim.html) at 2.5′ resolution (*c.* 5 km). For each species, we averaged the MAP for all occurrence points and then classified the species habitat as hydric ($MAP > 2000$ mm), mesic (500 mm $< MAP \leq 2000$ mm), or arid ($MAP \leq 500$ mm).

Statistical analysis

To investigate how leaf conduits' T and D_{max} scale to each other, we $\log_{10}$-transformed both variables and then used the

SMATR R-package v.3 (Warton *et al.*, 2012) to fit standardized major axis (SMA) regression models. We used the functions sma ($\log(T)$ *c.* $\log(D)$, slope.test = 1) to test whether the coefficient b for all species together was significantly different from one. To investigate whether the coefficients b ($\log(T)$ *c.* $\log(D) \times$ group) and a ($\log(T)$ *c.* $\log(D)$ + group) differed across groups (species, clades, habitats, growth forms, leaf sizes, and vein orders), we used Likelihood ratio (λ) and Wald (W) statistics, respectively (Warton *et al.*, 2012). We also performed Kruskal–Wallis tests followed by pairwise Wilcox tests with Benjamini & Hochberg's (1995) P-value adjustment method to test for differences in anatomical traits across those groups. Currently, the SMATR package does not support multiple regressions (Warton *et al.*, 2012). Thus, to investigate any potential influence of both leaf sizes and species in the T *c.* D scaling relationship across vein orders, we fitted a standard mixed model regression using the function 'lme' from the NLME R-package. Leaf area was model as fixed effect, while vein orders nested within species, and species nested within genus as random effects, that is lme ($\log(T)$ *c.* $\log(D) \times \log(\text{LA})$, random = *c.*1| genus/species/vein orders). We used the NLME function 'anova()' to assess the significance of each predictor variable effect and the function 'residplot()' from the PREDICTMEANS R-package to perform residual analysis.

To further examine phylogenetically driven variation in implosion safety, we built a phylogenetic tree for all species using V.PHYLOMAKER2 R-package (Jin & Qian, 2022) and the ' GBOTB.extended.WP.tre' mega-tree. Next, we used the function 'fastAnc' from the PHYTOOLS R-package to perform a fast estimation of the ancestral states for a, b, and T/D. We also conducted Blomberg's K tests (Blomberg *et al.*, 2003) using the PHYTOOLS function 'phylosig' to test for phylogenetic signals in those same traits (i.e. the tendency for related species to resemble each other, more than they resemble species drawn at random from a tree). $K < 1$ indicates faster trait evolution than expected under a Brownian model (weaker phylogenetic signal), while $K > 1$ indicates slower trait evolution (stronger phylogenetic signal).

To investigate possible trade-offs among leaf functions, we used two complementary approaches. First, we carried out a principal component analysis (PCA) using the 'prcomp' function in R. Before the PCA, we centered and z-transformed all traits to improve comparability among them and reduce bias toward traits with higher variance. We used the broken stick method (Jackson, 1993) for estimating the number of principal components to be retained. Our PCA was carried out with 106 of the 122 studied species, as we removed 16 species with missing data for VTotV and ε. Second, we ran ordinary least-squares regression models to test for pairwise trade-offs between implosion safety (response variable) and the other leaf traits (predictor variables). We also regressed P_{cri1} and P_{cri2} values to assess the relationship between our two different models of conduit collapse.

All analyses were carried out using the R v.4.3.1 (R Core Team, 2023). Code to reproduce analyses is available at https://github.com/ilamatos/xylem_implosion_safety. Regressions or differences were considered significant if $P < 0.05$.

Results

We measured 7113 leaf conduits. Conduit shape, dimensions, and arrangement greatly varied across species (Fig. 2; Table S1). Only 0.7% of the conduits exhibited ovality $O < 0.005$. The median critical pressure for collapse under hooping forces were −0.83 MPa (P_{cri1} low) and −2.40 MPa (P_{cri1} high), for the low and up ranges of xylem elastic modulus. Critical pressures for collapse due to radial forces were −3.92 MPa (P_{cri2} low) and −31.37 MPa (P_{cri2} high) for the low and up ranges of cell wall strength. P_{cri1} vs P_{cri2} were monotonically and nonlinearly correlated (Fig. S2a,b), and P_{cri2} always estimated more negative pressures for collapse (Fig. S2c–f). Median D_{max} was 6.90 µm, ranging from 1.21 µm (*Randia laetevirens* Standl., a dry tropical forest tree) to 80.28 µm (*Parajubaea torallyi* (Mart.) Burret, a dry tropical forest palm), whereas median T was 2.28 µm, ranging from 0.46 µm (*Sagittaria latifolia*, a temperate aquatic herb) to 7.95 µm (*Simmondsia chinensis* (Link) C.K.Schneid., a desert shrub). T/D varied *c.* 145-fold from 0.02 (*S. latifolia*) to 2.97 (*S. chinensis*). We also found substantial variation in functional traits across species (Table S1).

A negative allometry exists between leaf conduits diameter and thickness, but differences exist among clades

When we evaluated all species together, b was significantly lower than one ($b = 0.55$, test statistic $r = -0.58$, $P < 0.001$), indicating a negative allometry (Fig. 3). Both coefficients b (likelihood ratio statistic $\lambda = 672.6$, $P < 0.001$) and a (Wald statistic $W = 4284$, $P < 0.001$) significantly varied across species, ranging from $b = 0.29$–1.20 (Figs 4, S3) and $a = -0.77$ to 0.27 (Fig. S3; Table S2).

Despite the overall negative allometry (Fig. 4a), eight species (Table S2; Fig. 4b,c) showed b values not significantly different from one (isometric allometry), meaning a constant implosion safety across conduits of different sizes. None of the evaluated species showed $b > 1$ (positive allometry). Coefficients a ($W = 790.1$, $P < 0.01$) and b ($\lambda = 26.28$, $P < 0.01$) also significantly varied across plant clades (Fig. 5a–f). Asterids exhibited the thickest conduits with higher implosion safety ratios (T/D), while monocots showed the widest and thinnest conduits with smaller T/D (Fig. 6b; Table S3). K values were lower than 1 for T/D ($K = 0.33$; $P = 0.46$), a ($K = 0.62$; $P < 0.01$), and b ($K = 0.61$; $P < 0.01$), indicating weak phylogenetic signal for implosion safety. Ancestral reconstruction characters mapped onto the phylogenetic tree are shown in Figs 6(a), S4 and S5.

Leaf conduits are more resistant against implosion in arid habitats, woody species, small leaves, and minor veins

Coefficients a ($W = 349.6$, $P < 0.001$) and b ($\lambda = 10.92$, $P = 0.004$) varied across species habitats. Compared with hydric and mesic species, arid species showed significantly narrower and thicker conduits, with higher T/D (Table S3; Fig. 5g–i). Comparing across growth forms (Fig. S6), a ($W = 441.20$, $P < 0.01$) and b ($\lambda = 97.49$, $P < 0.01$) also varied significantly. Shrubs showed the narrower and potentially safer conduits (highest T/D ratios),

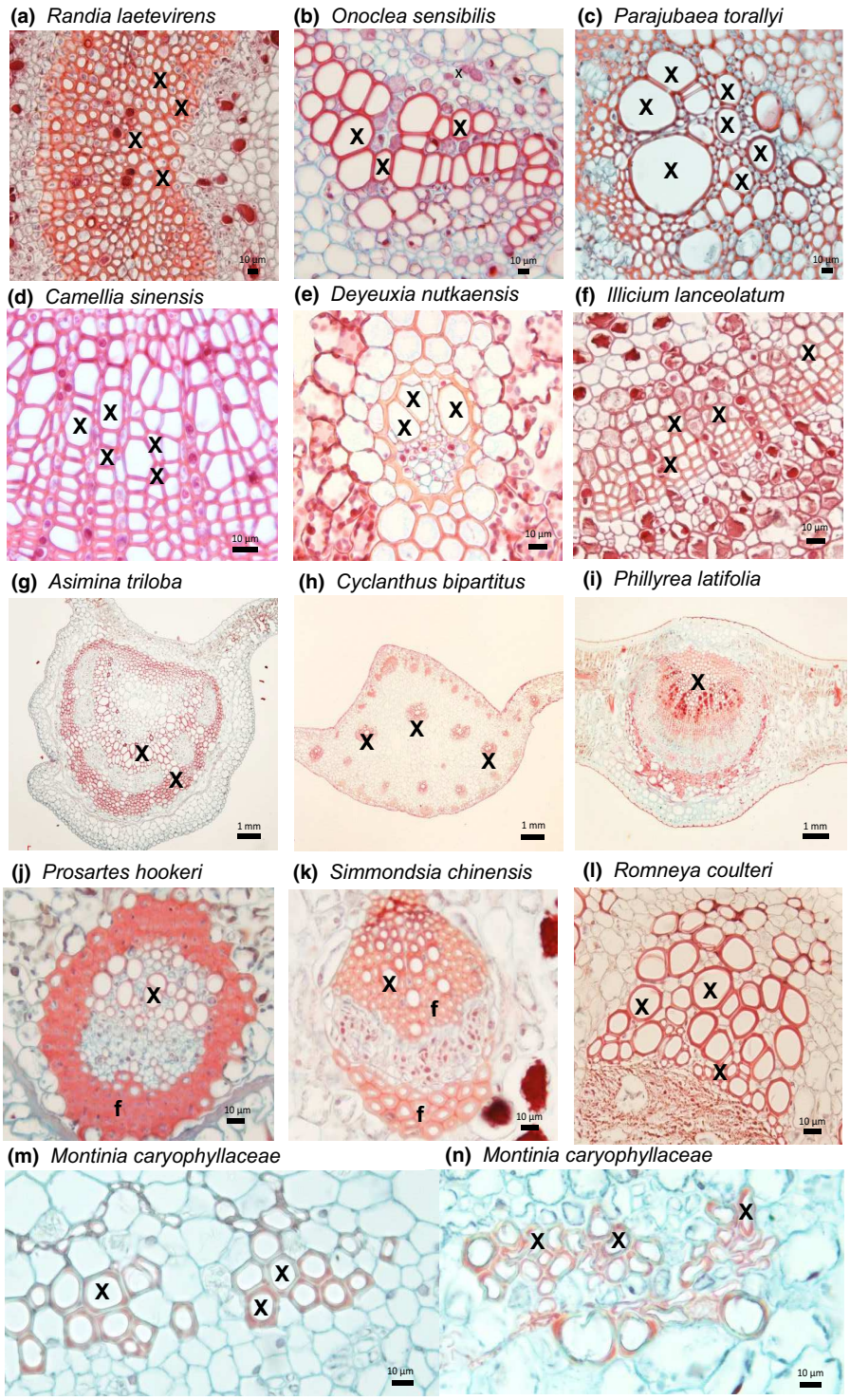

Fig. 2 Leaf cross-sectional images showing variation in the dimensions, shape, number, and arrangement of leaf xylem conduits (tracheids and vessel elements) across ferns and angiosperm species. (a) *Randia laetevirens* Standl. (asterid): mesic tree with narrow conduits; (b) *Onoclea sensibilis* L. (fern): mesic herb with medium size conduits; (c) *Parajubaea torallyi* (Mart.) Burret (monocot): mesic palm with wide conduits; (d) *Camellia sinensis* (L.) Kuntze (asterid): mesic tree with conduits of different shapes; (e) *Deyeuxia nutkaensis* (J.Presl) Steud. (monocot): mesic herb with ellipsoidal conduits; (f) *Illicium lanceolatum* A.C.Sm. (basal angiosperm): mesic tree with conduits of different shapes; (g) *Asimina triloba* (L.) Dunal (basal angiosperm): mesic tree, midrib with two layers of xylem conduits; (h) *Cyclanthus bipartitus* Poit. ex A.Rich. (monocot): hydric tree, midrib with many vascular bundles; (i) *Phillyrea latifolia* L. (asterid): mesic tree, midrib with single vascular bundle; (j) *Prosartes hookeri* Torr. (monocot): mesic herb, fibers surrounding the xylem conduits; (k) *Simmondsia chinensis* (Link) C.K.Schneid. (rosid): arid shrub, fibers intermingled with xylem conduits; (l) *Romneya coulteri* Harv. (basal eudicot): arid shrub, no apparent fiber neighboring xylem conduits; (m) *Montinia caryophyllacea* Thunb. (asterid): arid shrub: uncollapsed xylem conduits; (n) *Montinia caryophyllacea* (asterid): collapsed xylem conduits likely due to water stress. In all panels, some representative xylem conduits are labeled with X, while fibers, if present, are labeled with f. Only in panel n, the label X indicates collapsed xylem conduits, which can be identified by their irregular shape.

whereas aquatic species showed the wider and most vulnerable ones (lowest *T/D* ratios, Table S3). Implosion safety was higher, P_{cri} was lower (more negative), and b coefficient ($\lambda = 21.90$, $P < 0.01$) was steeper in microphyllous species (Table S3; Fig. S7), suggesting that conduits in small leaves are more resistant to implosion. However, our mixed model regression suggests a non-significant effect of leaf area on the *T c. D* scaling across vein orders (Table S4). Coefficients a ($W = 167$, $P < 0.001$) and b ($\lambda = 32.29$, $P < 0.001$) also differed across vein orders (Fig. 5j–l). Slope was significantly steeper (higher b) in minor and medium veins and shallower (lower b) in major veins, implying that conduit double-wall thickness increases with increasing diameter at a higher rate in higher vein orders than in major veins. Moreover, implosion safety index (*T/D* ratio) significantly increases from minor to major veins (Table S3), suggesting again that conduits in smaller veins might be more resistant to implosion.

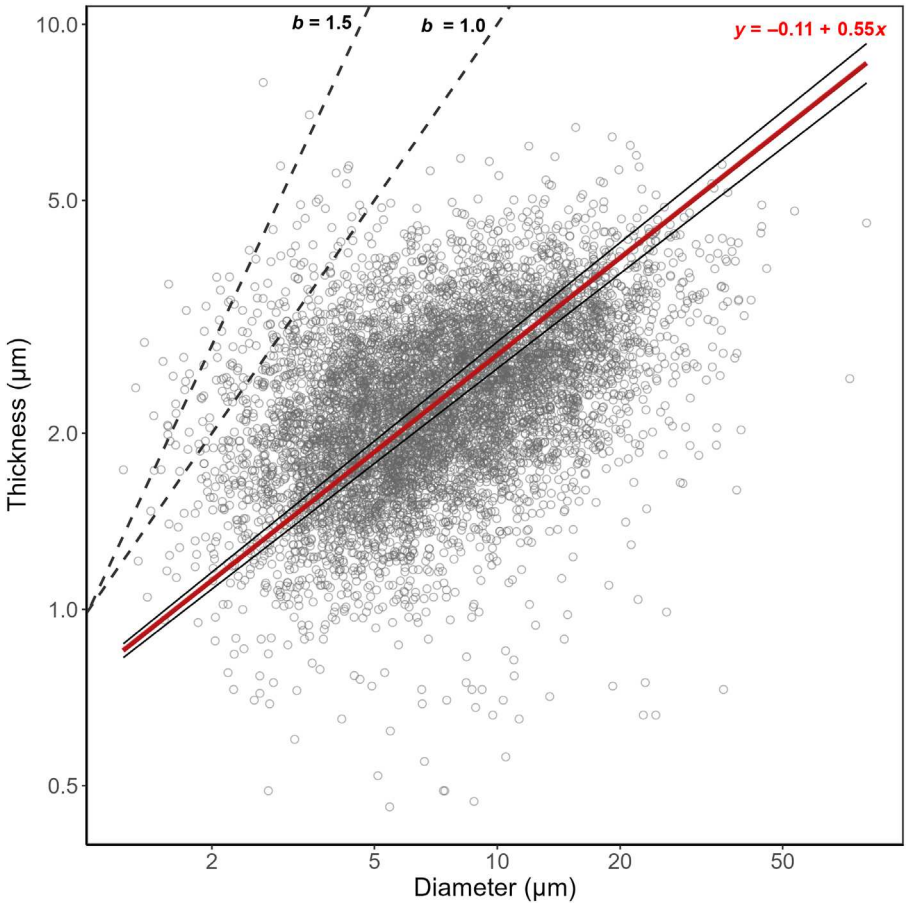

Fig. 3 Standardized major axis (SMA) regression for the log–log relationship between leaf conduit double-wall thickness and maximum lumen diameter across 7113 conduits measured from 122 species of fern and angiosperms. Values were $\log_{10}$-transformed before SMA regression, and then *xy*-axis were back transformed to their original units in μm. Black dashed lines indicate hypothetical isometric slope ($b = 1.0$) and positive allometric ($b = 1.5$) linear relationships between *T* vs *D*. Solid red line represents the actual estimated *T* vs D_{max} relationship, which conforms with a negative allometric relationship ($b = 0.55$; $a = -0.11$). Solid and thin black lines represent the 95% confidence interval for the SMA regression.

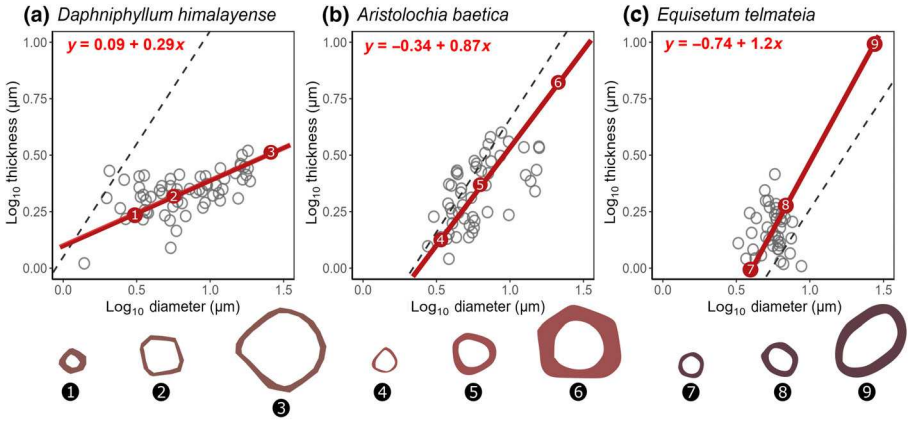

Conduit	1	2	3	4	5	6	7	8	9
D_{max} (μm)	3.54	5.62	25.12	3.54	5.62	25.12	3.54	5.62	25.12
T (μm)	1.80	2.05	3.17	1.38	2.07	7.58	0.83	1.46	8.90
T/D	0.51	0.36	0.12	0.39	0.37	0.30	0.24	0.26	0.35
P_{cri1} (MPa)	3.54	1.32	0.05	1.61	1.35	0.74	0.36	0.47	1.20
P_{cri2} (MPa)	10.28	5.34	0.63	6.10	5.40	3.64	2.23	2.70	5.02

Fig. 4 Standardized major axis regressions for the log–log relationship between leaf conduit double-wall thickness and maximum lumen diameter for three species with distinct slopes: (a) *Daphniphyllum himalayense* Müll.Arg. – negative allometry ($b = 0.29$, $a = 0.09$); (b) *Aristolochia baetica* L. – isometric allometry ($b = 0.87$ but not significantly different from 1, $a = -0.34$); and (c) *Equisetum telmateia* Ehrh. – isometric allometry ($b = 1.2$ but not significantly different from 1, $a = -0.74$). Black dashed lines represent an isometric line ($b = 1.0$). Numbered inserts illustrate the expected variation in conduits dimensions (D_{max}, maximum lumen diameter; *T*, double-cell wall thickness), implosion safety (*T/D*), critical pressure for implosion (P_{cri1} low and P_{cri2} low) according to their allometric equations. Conduit shapes approximate the real geometry observed in each species.

No trade-offs were observed between implosion safety, efficiency, and mechanical support

We identified two significant principal component (PC) axes (Fig. S8), which cumulatively explained 52% of the total variation among leaf traits (Fig. 7). PC1 was dominated by cost (LMA), implosion safety (*T/D*), and flow efficiency ($Kleaf_{max}$), while PC2 was associated with mechanical support (ε) and cost (VTotV). We found no evidence that higher implosion safety is linked to lower flow efficiency or higher mechanical support along the first two

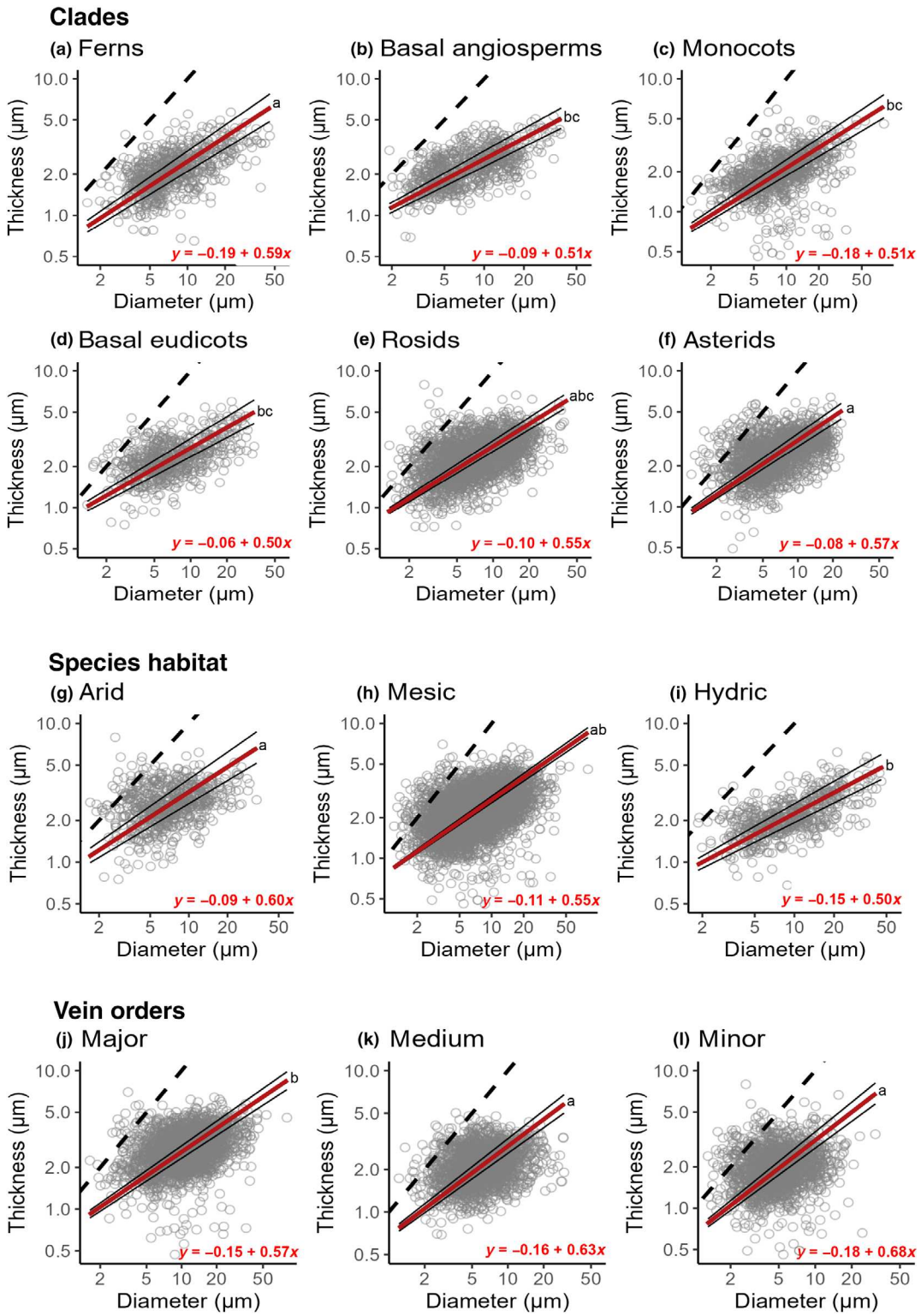

Fig. 5 Standardized major axis (SMA) regressions for the log–log relationship between leaf conduit double-wall thickness and maximum lumen diameter across clades: (a) ferns ($b = 0.59$, $a = -0.19$), (b) basal angiosperms ($b = 0.51$, $a = -0.09$), (c) monocots ($b = 0.51$, $a = -0.18$), (d) basal eudicots ($b = 0.50$, $a = -0.06$), (e) rosids ($b = 0.55$, $a = -0.10$), (f) asterids ($b = 0.57$, $a = -0.08$); species habitats: (g) arid ($b = 0.60$, $a = -0.09$), (h) mesic ($b = 0.55$, $a = -0.11$), (i) hydric ($b = 0.50$, $a = -0.15$); and vein orders: (j) major ($b = 0.57$, $a = -0.15$), (k) medium ($b = 0.63$, $a = -0.16$), (l) minor veins ($b = 0.68$, $a = -0.18$). Values were $\log_{10}$-transformed before SMA regression, and then *xy*-axis were back transformed to their original units in µm. Black dashed lines represent hypothetical isometric ($b = 1.0$) linear relationships between *T* vs *D*, with a zero *y*-intercept ($a = 0$). Solid red lines represent the actual estimated *T* vs *D* relationship. Solid and thin black lines represent the 95% confidence interval for the SMA regression. Letters indicate significant differences in the slopes across groups.

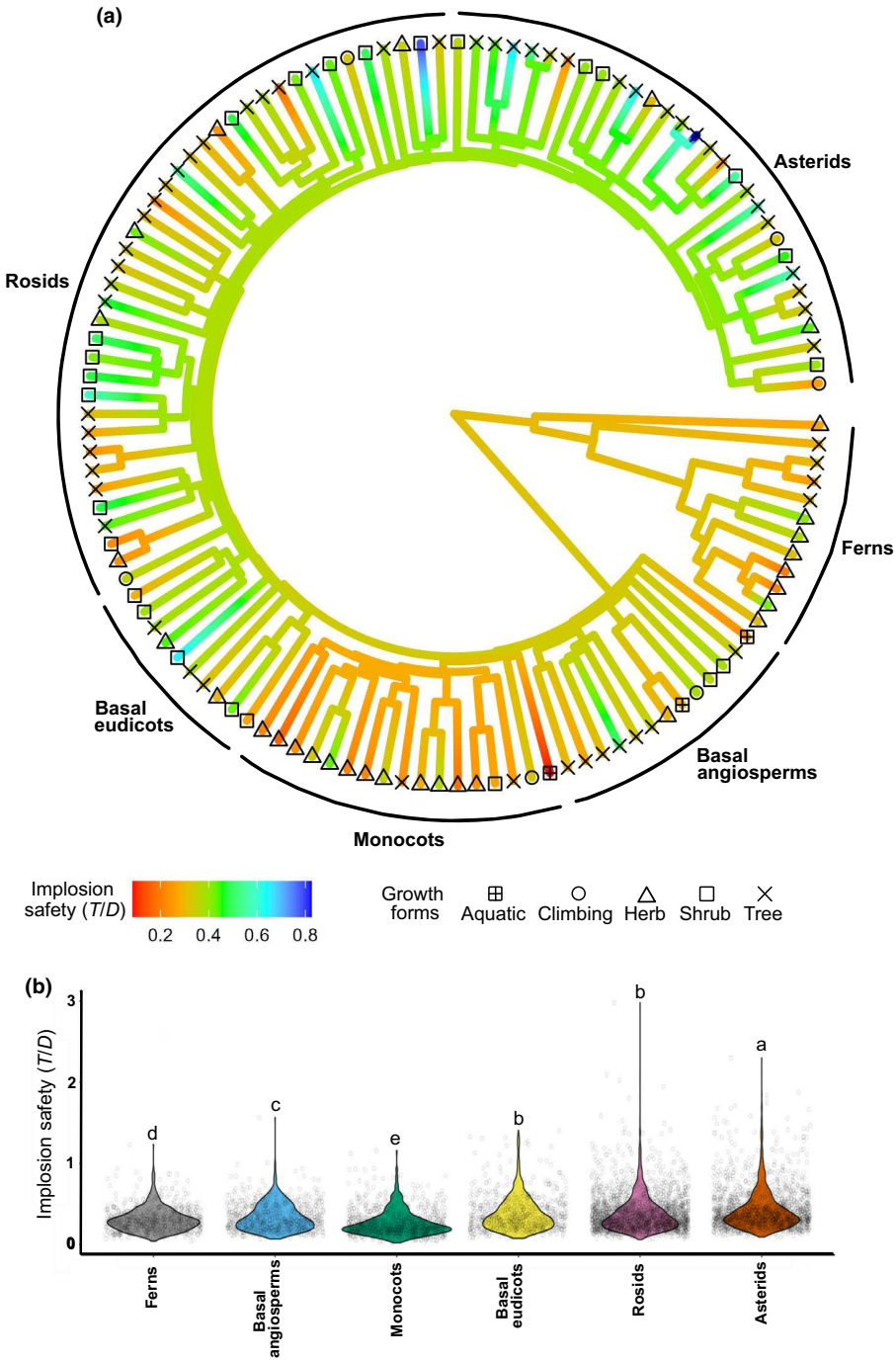

Fig. 6 Phylogenetically driven variation in implosion safety: (a) Ancestral state reconstruction of implosion safety ratio (T/D) for a phylogenetic tree of 122 species of ferns and angiosperms. Tip symbols indicate distinct growth forms (aquatic, climbing, herb, shrub, and tree). (b) Variation in T/D across plant clades. Letters indicate significant differences across groups according to Kruskal–Wallis tests followed by pairwise Wilcox tests.

PCs. Linear regressions corroborate those findings, as no significant trade-off was observed between implosion safety and flow efficiency, nor between safety and mechanical support (Fig. 8a,b). Higher safety against implosion was associated with higher construction cost described as LMA (Fig. 8c), but no significant relationship was found between implosion safety and VTotV (Fig. 8d).

Discussion

Overall, leaf conduits in ferns and angiosperms become wider faster than thicker, showing a negative allometry ($b < 1$). This negative allometry previously reported for 26 Australian woody angiosperms (Blackman *et al.*, 2018), is now confirmed within a much broader and more phylogenetically diverse dataset. Specifically, we found that conduit thickening is occurring at approximately half of the rate ($b = 0.55$) of proportional growth between T and D. This result indicates that (1) wider conduits are proportionally thinner for their diameter size, and hence potentially more vulnerable to implosion, whereas (2) narrower conduits are proportionally thicker for their diameter size, and hence potentially safer. If the tension inside xylem conduits was constant across the leaf venation network, we could expect an isometric scaling between T and D

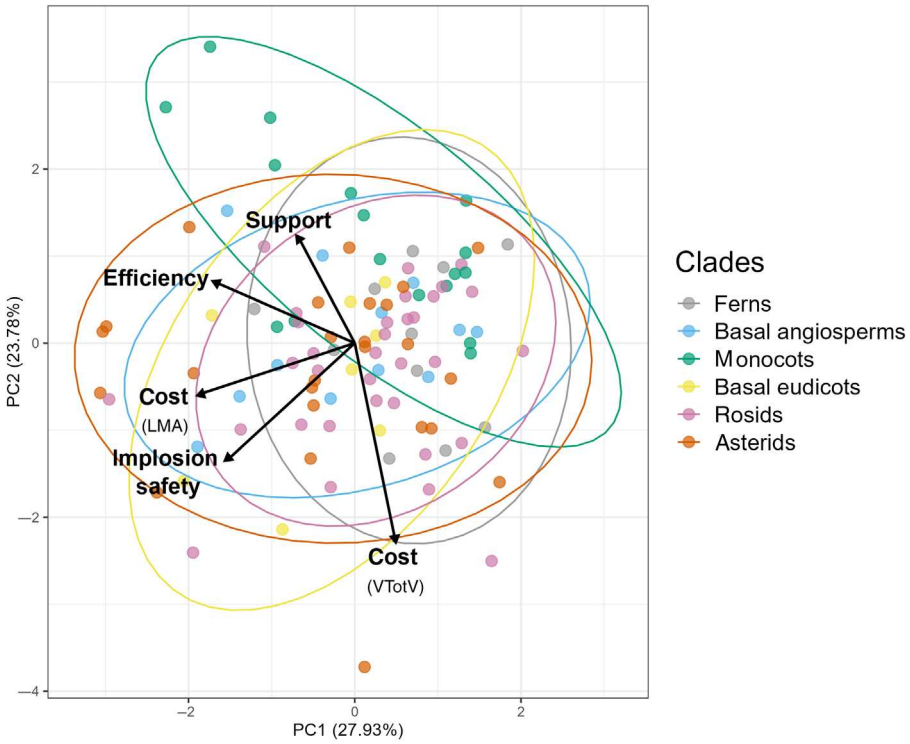

Fig. 7 Principal components analysis (PCA) of four leaf functional traits: conduit safety against implosion, flow efficiency, mechanical support, and construction cost in 108 ferns and angiosperms species (14 species were removed from the PCA because they missed values for mechanical support). 95% Confidence ellipses enclose the data at each plant clade. Parenthetical values indicate variance explained by each principal component. Implosion safety was described as the ratio between the leaf xylem conduits double-cell wall thickness and maximum lumen diameter; flow efficiency was quantified as the maximum lead hydraulic conductance; mechanical support was described as the leaf modulus of elasticity; and leaf construction cost was quantified as the leaf mass per area (LMA), and total volume of vein per unit of leaf area (VTotV).

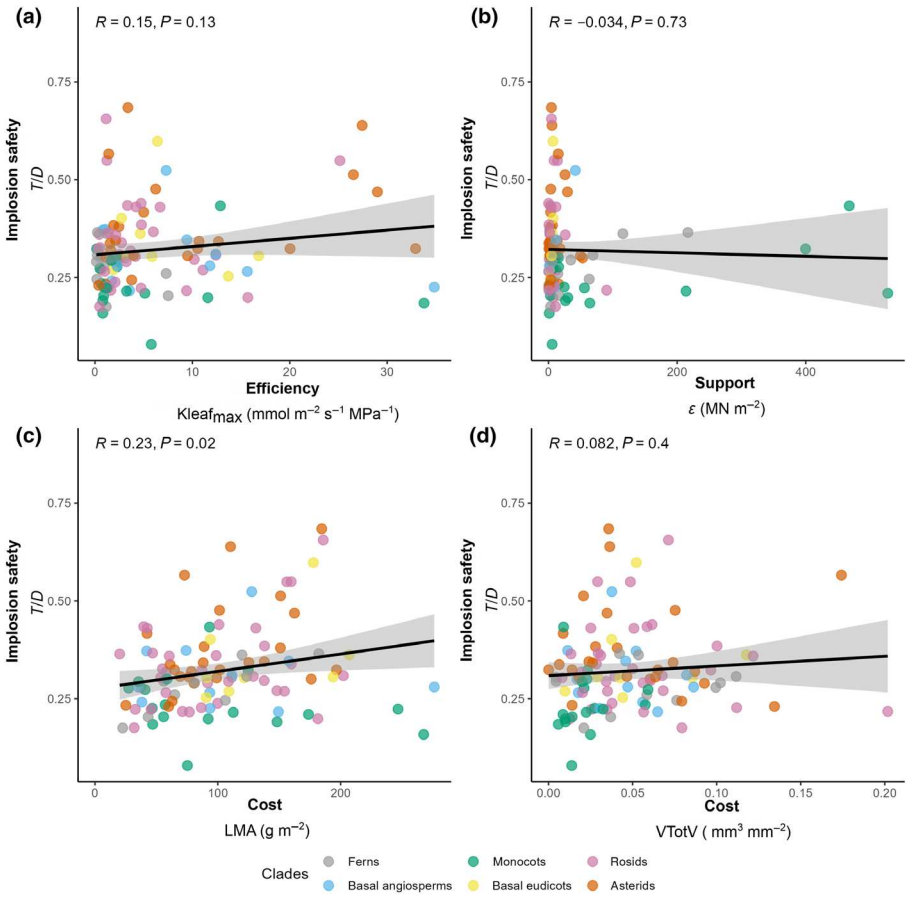

Fig. 8 Results of linear regression to test for pairwise trade-offs between four leaf functional traits: conduit safety against implosion (*T/D* – conduit thickness-to-span ratio), flow efficiency (Kleaf$_{max}$ – maximum leaf hydraulic conductance), mechanical support (ε – leaf flexural modulus of elasticity), and construction cost described either as leaf mass per area (LMA) or total volume of veins per unit of leaf area (VTotV), in 122 ferns and angiosperms species. (a) Implosion safety vs flow efficiency. (b) Implosion safety vs mechanical support. (c) Implosion safety vs cost, as described by LMA. (d) Implosion safety vs cost, as described by VTotV. In all panels, shaded areas indicate the 95% confidence interval of the linear regressions.

($b = 1$), reflecting a constant degree of implosion safety from larger to smaller veins. However, because xylem tension tends to increase, while conduits diameter tends to decrease (although sometimes 'enlarged' xylem conduits occur in terminal veins, e.g. Tucker, 1964), from the petiole to the minor veins (Coomes *et al.*, 2008), it makes sense for leaves to invest in higher implosion safety in the narrower conduits located at the more distal parts of the venation networks (i.e. minor veins). Such conduits are under higher risk of reaching critical pressures for collapse, especially when transpiring leaves are under water stress. By contrast, wider conduits located at proximal points (i.e. petiole and major veins) are usually under lower tension, and hence at lower risk of implosion. Thus, it might not be cost-effective to reinforce such larger conduits with enough lignin (Cochard *et al.*, 2004; Echeverría *et al.*, 2022) to achieve a proportional thickness to diameter ratio, that is to maintain a constant implosion safety across the entire venation network ($b = 1$).

Moreover, having wider, thinner, and potentially unsafe conduits could be evolutionarily viable in some cases. In our study, the least safe conduits (lowest *T/D*) were found in *S. latifolia*, an aquatic herb that is unlikely to be exposed to water potentials negative enough to cause implosion. It is also possible that leaves have collapsible conduits that implode under drought but quickly uncollapse after rehydration (Brodribb & Holbrook, 2005). Thus, elastic conduit implosion could also have adaptive significance in some circumstances. Assuming that the cell wall remains elastic during the implosion, the recovery from wall collapse could occur while pressures are still largely negative, contrary to cavitation-induced dysfunction that require positive pressure or metabolic energy to refill the conduits (Brodribb & Holbrook, 2005). Quickly reversible implosion has been observed in minor veins of conifer and angiosperm leaves (Cochard *et al.*, 2004; Chin *et al.*, 2022; Zhang *et al.*, 2023), and may function as a 'circuit breaker' to protect upstream conduits from embolisms (Zhang *et al.*, 2016, 2023) and/or as a water storage mechanism to buffer water potential changes in response to slow dehydration or vapor pressure deficit oscillations (Brodribb & Holbrook, 2005; Chin *et al.*, 2022).

When we compared *T* vs *D* scaling across vein orders, we found that minor veins were proportionally safer against implosion than major veins. This result corroborates the idea of a variable implosion safety across the venation network, but partially contradicts Blackman *et al.* (2018), who reported no statistically significant variation in scaling across vein orders, despite the existence of a negative allometry between *T* vs *D* in their dataset. Interestingly, minor veins seem to also be more resistant against embolisms (Brodribb *et al.*, 2016), so there could be an evolutionary coordination of strategies for defending xylem conduits against both implosion and cavitation (Sperry *et al.*, 2006; Bouche *et al.*, 2014). In this study, we did not directly observe collapse events, so we cannot rule out that our hypothetical predictors of implosion safety based on *T/D* might be insufficient to estimate the collapsibility of minor and major veins. For instance, xylem in major veins is often more structurally reinforced by surrounding fibers (Blackman *et al.*, 2010). This extra mechanical reinforcement (Kawai & Okada, 2016; Blonder *et al.*, 2020) may increase major veins implosion safety beyond that predicted solely by *T* and *D*. Contrarily, minor veins are usually leakier (Ohtsuka *et al.*, 2018), and the pit pores properties that increase their leakage could also weaken cell walls (Hacke *et al.*, 2004; Sperry & Hacke, 2004), decreasing implosion safety.

The examples above suggest that other features besides *T* and *D* could be important to determine implosion safety. Irregular conduit shapes can create areas in the conduit that are structurally weaker and prone to collapse at less negative pressures compared with a conduit of similar *T/D* and a more circular shape (Cochard *et al.*, 2004; Brodribb & Holbrook, 2005). Conduit length was not measured in this study; hence, we were unable to assess its potential influence on implosion safety. We also did not assess how pit pore features may affect P_{cri}. Estimates of implosion safety in wood xylem suggest that the presence of pit pores can weaken the double-cell walls reducing P_{cri} by 20–40% (Hacke *et al.*, 2004; Sperry & Hacke, 2004). But it is unclear whether those estimations are also valid for leaves. We recommend future studies to simultaneously measure those different conduit anatomical features (*D*, *T*, shape, length, number and size of pit pores) in a diverse set of species so that we will be able to partition their individual influences in P_{cri}.

Implosion safety can also be influenced by characteristics beyond the conduit level. For instance, at the vascular bundle level, the number of conduits, their arrangement, and the identity of their neighboring cells could all affect P_{cri}. Particularly in angiosperm leaves, fibers can surround conduit clusters (Fig. 2j, k) and help with resisting implosion (Sperry & Hacke, 2004). Contrastingly, xylem conduits attached to living cells (e.g. mesophyll cells) could be more prone to collapse under drought, particularly if living cells experience negative turgor pressure (Ding *et al.*, 2014). At the whole-leaf level, implosion safety might be increased by placing wide-thin-unsafe conduits in the center of the vascular bundle, where they are more protected against compressive forces; and arranging the narrow-thick-safe conduits at the periphery of the vascular bundle, where there is greater pressure for collapse (Sperry, 2003; Cochard *et al.*, 2004; e.g. Fig. 2c,l).

A mechanical model of implosion that explicitly considers all those features at the pit pore, conduit, vascular bundle, and whole-leaf levels remains to be developed. Not surprisingly, our models (P_{cri1}; P_{cri2}) estimated that implosion could occur at a large range of water potentials (Fig. S2). A great source of uncertainty in both of our models refers to cell wall elasticity (*E*) and strength (*W*) (Sperry & Hacke, 2004; Blackman *et al.*, 2010), which have been reported for xylem wood, but are still largely unknown for leaf xylem. All else being equal, conduits with stronger (higher *W*) and less elastic (higher *E*) cell walls should achieve more negative P_{cri}, hence higher resistance to collapse. This means that conduits with the same *T/D* ratio could differ in their actual P_{cri} due to differences in *E* and *W*, which are ultimately related to variation in the amount and spatial organization of the different materials (cellulose, hemicelluloses, and lignin) composing the secondary walls (Karam, 2005; Zhong *et al.*, 2019). To advance our understanding of the mechanical processes underlying leaf conduit implosion we need more measurements of *E* and *W*, as well as more studies

relating modeled P_{cri} with the actual range of pressures at which conduits implode.

Despite the overall trend of a negative allometry between T and D, eight of our studied species (Table S2) showed a slope not significantly different from one. This result suggests that although uncommon, an isometric scaling is possible in some species. However, these species did not have any particular functional or structural features in common, instead they spanned different clades, growth forms, habits, and leaf sizes, and also varied in their values of functional and anatomical traits (Table S1). Additionally, no species showed a positive allometry. Perhaps, because having conduits that are 'too' wide and also 'too' thick, although geometrically possible, it is biologically unfeasible for most (if not all) plants, as leaves would be investing 'too' much resources to lignified wide conduits, which are the ones experiments lower tension, hence lower implosion risk.

When comparing a and b across plant clades, we could expect a trend of decreased implosion safety from more basal to more derived clades. This is because the evolution of xylem conduits from hydroids (in bryophytes) through tracheids (in most ferns and conifers) to vessels (in most angiosperms) reflects a general trend of increased D and decreased T, which should culminate in a trend of decreased implosion safety across clades (Sperry, 2003; Sperry *et al.*, 2006; Feild & Brodribb, 2013). However, our results do not clearly support this expectation. Asterids (a more derived angiosperm group) showed the thickest and safest conduits, whereas monocots (a more basal angiosperm group) showed the widest, thinnest, and least safe conduits. This reversed trend is somehow compatible with the 'aquatic origin' theory for angiosperms (Soltis *et al.*, 2008), which presumes that the first angiosperms were aquatic herbs that later diverged in terrestrial habitats. Because aquatic leaves are rarely (or never) subjected to water stress and can be partially or completely supported by the water, their conduits might become as wide as possible to maximize the hydraulic efficiency, without the need to invest much in mechanical support or implosion safety. In fact, in our dataset, aquatic species showed the least implosion resistant conduits (i.e. lower T/D ratios), whereas shrubs and trees showed higher values of implosion safety (i.e. higher T/D ratios). However, our data only included three aquatic species (two basal angiosperms and one basal monocot), so further studies are needed to elucidate the evolutionary trends of implosion safety across clades and growth forms. It is also possible that the apparent lower safety in monocot conduits is partially counteracted by the presence of a high density of fibers (Carlquist, 2012), which can increase resistance to buckling forces independent of conduit dimensions. In a recent study, leaf xylem implosion was observed in some monocot species (grass and bamboo) but not in others (bamboos and palm) despite the relatively large tensions (< -4.0 MPa) inside their conduits (Zhang *et al.*, 2023). This means that closely related species can differ in their levels of implosion resistance, which is corroborated by the low phylogenetic signals reported in our study for a, b and T/D. Collectively, those results suggest that the evolution of implosion safety was likely complex and nonlinear. Future studies examining xylem collapse in different types of conduits (tracheids and vessels) and secondary wall patternings (i.e. annular, helical, reticulate, scalariform, and pitted) will be necessary to better understand the evolutionary trends in implosion safety.

When comparing a and b across habitats, we could expect a trend of increased implosion safety in drier areas. Studies with both wood (Sperry & Hacke, 2004) and leaf xylem (Blackman *et al.*, 2018) have shown that wet environments favor species with wide and thin conduits, whereas dry environments favor species with narrow and thick conduits. Our present study confirmed those trends while also finding higher values of both a and b coefficients in species from arid habitats. Importantly, such differences persisted even when species were growing under the same climatic conditions in the botanical garden, suggesting low environmental plasticity in leaf conduit anatomical traits (Fonti & Jansen, 2012; Gričar *et al.*, 2015; Fontes *et al.*, 2022). The T vs D scaling also significantly varied across leaf sizes. Contrary to our expectations, higher implosion safety was observed in smaller leaves, perhaps because microphyllous species are commonly found in hot and arid environments (McDonald *et al.*, 2003), and so are under higher risk of conduit collapse than meso- and macrophyllous species.

Our overall finding that leaves are growing conduits wider than thicker suggests that species prioritize higher hydraulic efficiency (by producing wider conduits) and lower construction cost (by producing thinner conduits) over higher implosion safety and mechanical support. Nonetheless, we did not find strong trade-offs within the leaf functional traits examined. Even though those trade-offs might be true at the conduit level, when we scale them at the whole-leaf level, where the measurements of $Kleaf_{max}$, ε, and LMA were taken, they may weaken or even disappear. As discussed above, features such as the number and arrangement of leaf conduits and their interactions with neighboring cells could uncouple those trade-offs so that the implosion safety at the whole-leaf level cannot be easily predicted by the sum of the conduits individual resistances to collapse. Moreover, there could be complex nonlinear relationships between implosion safety, support, efficiency, and cost, which were not evaluated in this study. Limited knowledge of how xylem and non-xylem features vary within organisms also makes scaling implosion safety to whole organism function difficult. To fully describe leaf conduits' ability to resist collapse imposed by negative pressures, further studies need to investigate how surrounding elements (e.g. fibers and mesophyll.) influence implosion safety and other leaf functions.

Acknowledgements

We are grateful to all staff of the University of California Botanical Garden at Berkeley for the logistical support, especially horticulturists Ethan Fenner, Eric Hupperts, James Fong, Noah Gapsis, Gideon Dollarhide, Sophia Warsh, Jason Bonham, and Corina Rieder and Director of Research & Collections Vanessa Handley who helped us with sample collection. We thank Denise Schichnes for sharing histological and microscopy methods. We also thank Cynthia Looy and Todd E. Dawson for lending equipment to obtain the leaf anatomical dataset. Undergraduate

students that worked in this project were supported either by UC Berkeley programs: Undergraduate Research Apprentice Program (URAP) and Sponsored Projects for Undergraduate Research (SPUR), or by the United States National Science Foundation (NSF) programs: Research Experiences for Undergraduates (REU) and Research Experience for Post-Baccalaureate Students (REPS). This study was supported by the US National Science Foundation (grant DEB-2025282). All participants were supported by the United States National Science Foundation under grant DEB-2025282. DK, JT, SM, JW, and RS were also supported by University of California at Berkeley Sponsored Projects for Undergraduate Research (SPUR). LG was supported by United States National Science Foundation Research Experiences for Undergraduates (NSF-REU), and BCJ by NSF Research Experience for Post-Baccalaureate Students (NSF-REPS).

Competing interests

None declared.

Author contributions

ISM designed the study. BWB secured the funding. ISM, SM, DK and JR prepared and imaged the leaf cross-sectional slides. ISM, SM, BCJ, RS and JW analyzed the leaf cross-sectional images and manually measured the xylem conduits diameters and double-cell wall thickness. ISM, AF, JT, SC, LG and MB collected the leaf samples and measured the leaf functional traits. HF provided logistical support and access to the botanical garden living collections. ISM analyzed the data, led the manuscript writing and prepared the figures. All authors contributed to the manuscript draft.

ORCID

Benjamin Wong Blonder https://orcid.org/0000-0002-5061-2385
Mickey Boakye https://orcid.org/0000-0002-6557-9928
Holly Forbes https://orcid.org/0000-0001-7487-8068
Diana Kalantar https://orcid.org/0009-0009-2233-163X
Ilaine Silveira Matos https://orcid.org/0000-0001-5557-5133

Data availability

All data produced and used in this study, including leaf cross-sectional images, are publicly available on Dryad repository at https://doi.org/10.5061/dryad.b8gtht7mc. R-code to reproduce all analysis and figures is available at https://github.com/ilamatos/xylem_implosion_safety.

References

Amthor JS. 2003. Efficiency of lignin biosynthesis: a quantitative analysis. *Annals of Botany* **91**: 673–695.

Benjamini Y, Hochberg Y. 1995. Controlling the false discovery rate: a practical and powerful approach to multiple testing. *Journal of the Royal Statistical Society: Series B (Methodological)* **57**: 289–300.

Blackman CJ, Brodribb TJ, Jordan GJ. 2010. Leaf hydraulic vulnerability is related to conduit dimensions and drought resistance across a diverse range of woody angiosperms. *New Phytologist* **188**: 1113–1123.

Blackman CJ, Gleason SM, Cook AM, Chang Y, Laws CA, Westoby M. 2018. The links between leaf hydraulic vulnerability to drought and key aspects of leaf venation and xylem anatomy among 26 Australian woody angiosperms from contrasting climates. *Annals of Botany* **122**: 59–67.

Blomberg SP, Garland T Jr, Ives AR. 2003. Testing for phylogenetic signal in comparative data: behavioral traits are more labile. *Evolution* **57**: 717–745.

Blonder B, Both S, Jodra M, Xu H, Fricker M, Matos IS, Majalap N, Burslem DFRP, Teh YA, Malhi Y. 2020. Linking functional traits to multiscale statistics of leaf venation networks. *New Phytologist* **228**: 1796–1810.

Bouche PS, Larter M, Domec J-C, Burlett R, Gasson P, Jansen S, Delzon S. 2014. A broad survey of hydraulic and mechanical safety in the xylem of conifers. *Journal of Experimental Botany* **65**: 4419–4431.

Brodribb TJ, Bienaimé D, Marmottant P. 2016. Revealing catastrophic failure of leaf networks under stress. *Proceedings of the National Academy of Sciences, USA* **113**: 4865–4869.

Brodribb TJ, Holbrook NM. 2005. Water stress deforms tracheids peripheral to the leaf vein of a tropical conifer. *Plant Physiology* **137**: 1139–1146.

Carlquist S. 2012. Monocot xylem revisited: new information, new paradigms. *The Botanical Review* **78**: 87–153.

Chin ARO, Guzmán-Delgado P, Sillett SC, Kerhoulas LP, Ambrose AR, McElrone AR, Zwieniecki MA. 2022. Tracheid buckling buys time, foliar water uptake pays it back: coordination of leaf structure and function in tall redwood trees. *Plant, Cell & Environment* **45**: 2607–2616.

Choat B, Jansen S, Brodribb TJ, Cochard H, Delzon S, Bhaskar R, Bucci SJ, Feild TS, Gleason SM, Hacke UG *et al.* 2012. Global convergence in the vulnerability of forests to drought. *Nature* **491**: 752–755.

Cochard H, Froux F, Mayr S, Coutand C. 2004. Xylem wall collapse in water-stressed pine needles. *Plant Physiology* **134**: 401–408.

Coomes DA, Heathcote S, Godfrey ER, Shepherd JJ, Sack L. 2008. Scaling of xylem vessels and veins within the leaves of oak species. *Biology Letters* **23**: 302–306.

Ding Y, Zhang Y, Zheng Q-S, Tyree MT. 2014. Pressure–volume curves: revisiting the impact of negative turgor during cell collapse by literature review and simulations of cell micromechanics. *New Phytologist* **203**: 378–387.

Echeverría A, Petrone-Mendoza E, Segovia-Rivas A, Figueroa-Abundiz VA, Olson ME. 2022. The vessel wall thickness–vessel diameter relationship across woody angiosperms. *American Journal of Botany* **109**: 856–873.

Feild TS, Brodribb TJ. 2013. Hydraulic tuning of vein cell microstructure in the evolution of angiosperm venation networks. *New Phytologist* **199**: 720–726.

Fontes CG, Pinto-Ledezma J, Jacobsen AL, Pratt RB, Cavender-Bares J. 2022. Adaptive variation among oaks in wood anatomical properties is shaped by climate of origin and shows limited plasticity across environments. *Functional Ecology* **36**: 326–340.

Fonti P, Jansen S. 2012. Xylem plasticity in response to climate. *New Phytologist* **195**: 734–736.

Gričar J, Prislan P, De Luis M, Gryc V, Hacurová J, Vavrčík H, Čufar K. 2015. Plasticity in variation of xylem and phloem cell characteristics of Norway spruce under different local conditions. *Frontiers in Plant Science* **6**: 730.

Hacke UG, Sperry JS, Pittermann J. 2004. Analysis of circular bordered pit function II. Gymnosperm tracheids with torus-margo pit membranes. *American Journal of Botany* **91**: 386–400.

Hacke UG, Sperry JS, Pockman WT, Davis SD, McCulloh KA. 2001. Trends in wood density and structure are linked to prevention of xylem implosion by negative pressure. *Oecologia* **126**: 457–461.

Ikeda CM, Wilkerling J, Duncan JH. 2013. The implosion of cylindrical shell structures in a high-pressure water environment. *Proceedings of the Royal Society A: Mathematical, Physical and Engineering Sciences* **469**: 20130443.

Jackson DA. 1993. Stopping rules in principal components analysis: a comparison of heuristical and statistical approaches. *Ecology* **74**: 2204–2214.

Jin Y, Qian H. 2022. V.PHYLOMAKER2: an updated and enlarged R package that can generate very large phylogenies for vascular plants. *Plant Diversity* **44**: 335–339.

Johansen DA. 1940. *Plant microtechnique*. London, UK: McGraw-Hill Book, 530.

Karam GN. 2005. Biomechanical model of the xylem vessels in vascular plants. *Annals of Botany* **95**: 1179–1186.

Kawai K, Okada N. 2016. How are leaf mechanical properties and water-use traits coordinated by vein traits? A case study in Fagaceae. *Functional Ecology* **30**: 527–536.

Maitner BS, Boyle B, Casler N, Condit R, Donoghue J, Durán SM, Guaderrama D, Hinchliff CE, Jørgensen PM, Kraft NJB *et al.* 2018. The BIEN R package: a tool to access the Botanical Information and Ecology Network (BIEN) database. *Methods in Ecology and Evolution* **9**: 373–379.

McDonald PG, Fonseca CR, Overton JM, Westoby M. 2003. Leaf-size divergence along rainfall and soil-nutrient gradients: is the method of size reduction common among clades? *Functional Ecology* **17**: 50–57.

Melcher PJ, Michele Holbrook N, Burns MJ, Zwieniecki MA, Cobb AR, Brodribb TJ, Choat B, Sack L. 2012. Measurements of stem xylem hydraulic conductivity in the laboratory and field. *Methods in Ecology and Evolution* **3**: 685–694.

Nardini A. 2022. Hard and tough: the coordination between leaf mechanical resistance and drought tolerance. *Flora* **288**: 152023.

Ohtsuka A, Sack L, Taneda H. 2018. Bundle sheath lignification mediates the linkage of leaf hydraulics and venation. *Plant, Cell & Environment* **41**: 342–353.

Pérez-Harguindeguy N, Díaz S, Garnier E, Lavorel S, Poorter H, Jaureguiberry P, Bret-Harte MS, Cornwell WK, Craine JM, Gurvich DE *et al.* 2016. Corrigendum to: New handbook for standardised measurement of plant functional traits worldwide. *Australian Journal of Botany* **64**: 715.

Pittermann J, Limm E, Rico C, Christman MA. 2011. Structure-function constraints of tracheid-based xylem: a comparison of conifers and ferns. *New Phytologist* **192**: 449–461.

Pittermann J, Sperry JS, Wheeler JK, Hacke UG, Sikkema EH. 2006. Mechanical reinforcement of tracheids compromises the hydraulic efficiency of conifer xylem. *Plant, Cell & Environment* **29**: 1618–1628.

Pratt RB, Jacobsen AL. 2017. Conflicting demands on angiosperm xylem: tradeoffs among storage, transport and biomechanics. *Plant, Cell & Environment* **40**: 897–913.

R Core Team. 2023. *R: a language and environment for statistical computing.* Vienna, Austria: R Foundation for Statistical Computing. [WWW document] URL https://www.R-project.org/ [accessed 10 December 2023].

Read J, Sanson GD, Lamont BB. 2005. Leaf mechanical properties in sclerophyll woodland and shrubland on contrasting soils. *Plant and Soil* **276**: 95–113.

Růžička K, Ursache R, Hejátko J, Helariutta Y. 2015. Xylem development – from the cradle to the grave. *New Phytologist* **207**: 519–535.

Sack L, Scoffoni C. 2012. Measurement of leaf hydraulic conductance and stomatal conductance and their responses to irradiance and dehydration using the evaporative flux method (EFM). *Journal of Visualized Experiments* **70**: 4179.

Shipley B, De Bello F, Cornelissen JHC, Laliberté E, Laughlin DC, Reich PB. 2016. Reinforcing loose foundation stones in trait-based plant ecology. *Oecologia* **180**: 923–993.

Soltis DE, Bell CD, Kim S, Soltis PS. 2008. Origin and early evolution of angiosperms. *Annals of the New York Academy of Sciences* **1133**: 3–25.

Sperry JS. 2003. Evolution of water transport and xylem structure. *International Journal of Plant Sciences* **164**: S115–S127.

Sperry JS, Hacke UG. 2004. Analysis of circular bordered pit function I. Angiosperm vessels with homogenous pit membranes. *American Journal of Botany* **91**: 369–385.

Sperry JS, Hacke UG, Pittermann J. 2006. Size and function in conifer tracheids and angiosperm vessels. *American Journal of Botany* **93**: 1490–1500.

Timoshenko S. 1930. *Strength of materials.* London, UK: MacMillan.

Tucker SC. 1964. The terminal idioblasts in magnoliaceous leaves. *American Journal of Botany* **51**: 1051–1062.

Tyree MT, Davis SD, Cochard H. 1994. Biophysical perspectives of xylem evolution: is there a tradeoff of hydraulic efficiency for vulnerability to dysfunction? *IAWA Journal* **15**: 335–360.

Warton DI, Duursma RA, Falster DS, Taskinen S. 2012. SMATR 3 – an R package for estimation and inference about allometric lines. *Methods in Ecology and Evolution* **3**: 257–259.

Webb LJ. 1959. A physiognomic classification of Australian rain forests. *Journal of Ecology* **47**: 551–570.

Xu H, Blonder B, Jodra M, Malhi Y, Fricker M. 2021. Automated and accurate segmentation of leaf venation networks via deep learning. *New Phytologist* **229**: 631–648.

Young WC. 1989. *Roark's formulas for stress and strain.* New York, NY, USA: McGraw-Hill.

Zhang Y, Hochberg U, Rockwell FE, Ponomarenko A, Chen Y, Manandhar A, Graham AC, Holbrook NM. 2023. Xylem conduit deformation across vascular plants: an evolutionary spandrel or protective valve? *New Phytologist* **237**: 1242–1255.

Zhang Y-J, Rockwell FE, Graham AC, Alexander T, Holbrook NM. 2016. Reversible leaf xylem collapse: a potential "circuit breaker" against cavitation. *Plant Physiology* **172**: 2261–2274.

Zhang Y-J, Rockwell FE, Wheeler JK, Holbrook NM. 2014. Reversible deformation of transfusion tracheids in *Taxus baccata* is associated with a reversible decrease in leaf hydraulic conductance. *Plant Physiology* **165**: 1557–1565.

Zhong R, Cui D, Ye Z-H. 2019. Secondary cell wall biosynthesis. *New Phytologist* **221**: 1703–1723.

Zwieniecki MA, Melcher PJ, Boyce CK, Sack L, Holbrook NM. 2002. Hydraulic architecture of leaf venation in *Laurus nobilis* L. *Plant, Cell & Environment* **25**: 1445–1450.

Supporting Information

Additional Supporting Information may be found online in the Supporting Information section at the end of the article.

Fig. S1 Global map with coordinates of native occurrence for 122 species of ferns and angiosperms.

Fig. S2 Theoretical critical implosion pressures for leaf conduits implosion.

Fig. S3 Standardized major axis regressions for the $\log_{10}$–$\log_{10}$ relationship between leaf conduit cell double-wall thickness and lumen diameter.

Fig. S4 Ancestral state reconstruction of the slope between xylem conduit double-cell wall thickness and diameter.

Fig. S5 Ancestral state reconstruction of the *y*-intercept between xylem conduit double-cell wall thickness and diameter.

Fig. S6 Standardized major axis regression results across plant growth forms.

Fig. S7 Standardized major axis regression results across leaf sizes.

Fig. S8 Results for the broken stick method.

Table S1 List of 122 species of ferns and angiosperms collected from the University of California Botanical Garden at Berkeley.

Table S2 Results of the standardized major axis regressions.

Table S3 Results of Kruskal–Wallis tests followed by pairwise Wilcox tests.

Table S4 Results of a mixed model regression analysis.

Please note: Wiley is not responsible for the content or functionality of any Supporting Information supplied by the authors. Any queries (other than missing material) should be directed to the *New Phytologist* Central Office.